High Dominant Frequencies and Fractionated Potentials Do Not Indicate Focal or Rotational Activation During AF

van Staveren, Lianne N.; Hendriks, Richard C.; Taverne, Yannick J.H.J.; de Groot, Natasja M.S.

DOI
10.1016/j.jacep.2023.01.013

Publication date
2023

Document Version
Final published version

Published in
JACC: Clinical Electrophysiology

Citation (APA)
van Staveren, L. N., Hendriks, R. C., Taverne, Y. J. H. J., & de Groot, N. M. S. (2023). High Dominant Frequencies and Fractionated Potentials Do Not Indicate Focal or Rotational Activation During AF. *JACC: Clinical Electrophysiology*, *9*(7), 1082-1096. https://doi.org/10.1016/j.jacep.2023.01.013

JACC: CLINICAL ELECTROPHYSIOLOGY VOL. 9, NO. 7, 2023

PUBLISHED BY ELSEVIER

ORIGINAL RESEARCH

ATRIAL FIBRILLATION - MECHANISMS

High Dominant Frequencies and Fractionated Potentials Do Not Indicate Focal or Rotational Activation During AF

Lianne N. van Staveren, MD,[a] Richard C. Hendriks, PhD,[c] Yannick J.H.J. Taverne, MD, PhD,[b] Natasja M.S. de Groot, MD, PhD[a]

ABSTRACT

BACKGROUND Dominant frequencies (DFs) or complex fractionated atrial electrograms (CFAEs), indicative of focal sources or rotational activation, are used to identify target sites for atrial fibrillation (AF) ablation in clinical studies, although the relationship among DF, CFAE, and activation patterns remains unclear.

OBJECTIVES This study sought to investigate the relationship between patterns of activation underlying DF and CFAE sites during AF.

METHODS Epicardial high-resolution mapping of the right and left atrium including Bachmann's bundle was performed in 71 participants. We identified the highest dominant frequency (DF_{max}) and highest degree of CFAE ($CFAE_{max}$) with the use of existing clinical criteria and classified patterns of activation as focal or rotational activation and smooth propagation, conduction block (CB), collision and remnant activity, and fibrillation potentials as single, double, or fractionated potentials containing, respectively, 1, 2, or 3 or more negative deflections. Relationships among activation patterns, DF_{max}, and potential types were investigated.

RESULTS DF_{max} were primarily located at the left atrioventricular groove and did not harbor focal activation (proportion focal waves: 0% [IQR: 0%-2%]). Compared with non-DF_{max} sites, DF_{max} were characterized by more frequent smooth propagation (22% [IQR: 7%-48%] vs 17% [IQR: 11%-24%]; $P = 0.001$), less frequent conduction block (69% [IQR: 51%-81%] vs 74% [IQR: 69%-78%]; $P = 0.006$), a higher proportion of single potentials (72% [IQR: 55%-84%] vs 6%1 [IQR: 55%-65%]; $P = 0.003$), and a lower proportion of fractionated potentials (4% [IQR: 1%-11%] vs 12% [IQR: 9%-15%]; $P = 0.004$). $CFAE_{max}$ were mainly found at the pulmonary veins area, and only 1% [IQR: 0%-2%] of all $CFAE_{max}$ contained focal activation. Compared with non-$CFAE_{max}$ sites, $CFAE_{max}$ sites were characterized by less frequent smooth propagation (1% [IQR: 0%-1%] vs 17% [IQR: 12%-24%]; $P < 0.001$) and more frequent remnant activity (20% [IQR: 12%-29%] vs 8% [IQR: 5%-10%]; $P < 0.001$), and harbored predominantly fractionated potentials (52% [IQR: 43%-66%] vs 12% [IQR: 9%-14%]; $P < 0.001$).

CONCLUSIONS Focal or rotational patterns of activation were not consistently detected at DF_{max} domains and $CFAE_{max}$ sites. These findings do not support the concept of targeting DF_{max} or $CFAE_{max}$ according to existing criteria for AF ablation. (J Am Coll Cardiol EP 2023;9:1082-1096) © 2023 by the American College of Cardiology Foundation.

From the [a]Department of Cardiology, Erasmus Medical Center, Rotterdam, the Netherlands; [b]Department of Cardiothoracic Surgery, Erasmus Medical Center, Rotterdam, the Netherlands; and the [c]Delft University of Technology, Delft, the Netherlands.
The authors attest they are in compliance with human studies committees and animal welfare regulations of the authors' institutions and Food and Drug Administration guidelines, including patient consent where appropriate. For more information, visit the Author Center.

Manuscript received March 14, 2022; revised manuscript received January 19, 2023, accepted January 23, 2023.

ISSN 2405-500X/$36.00 https://doi.org/10.1016/j.jacep.2023.01.013

Success rates of pulmonary vein (PV) isolation in patients with persistent atrial fibrillation (AF) remain moderate despite development of adjunctive ablation strategies targeting atrial sites considered to be crucial to AF perpetuation. These sites harbor complex fractionated atrial electrograms (CFAEs)[1] or so-called focal sources driving AF identified by dominant frequencies (DFs). However, ablative therapy targeting either CFAEs or DFs in large study populations did not improve arrhythmia-free survival.[2-6] The CFAE ablation strategy has been largely abandoned, because CFAEs are recorded during slowing of conduction, pivoting around lines of conduction block or nearby focal sources and therefore they may not be specific enough for the substrate perpetuating AF.

DF mapping is used to identify AF sources, but with mixed outcomes. Recent mapping studies in patients with paroxysmal and persistent AF reported that fewer than 4% of DF sites corresponded to rotational activity or focal sources.[7] An important limitation of mapping studies performed so far is the use of endovascular mapping techniques, which hampers detailed analysis of activation patterns caused by the relatively large interelectrode distances[8] and instability of the catheter tip position. In addition, mapping studies have been frequently focused on isolated atrial regions. Consequently, the relationship among focal sources, high DF sites, and nearby CFAE sites remains unclear. We hypothesized that if a relationship among DFs, CFAEs, and AF sources would exist, high-resolution mapping of the right (RA) and left atrium (LA) would be able to detect it. The goal of the present study was, therefore, to investigate the relationship between patterns of activation underlying DF and CFAE sites by constructing high-resolution epicardial maps derived from the RA and LA, including Bachmann's bundle (BB), during AF.

METHODS

STUDY POPULATION. The study population included patients admitted for elective surgical correction of ischemic, valvular, or congenital heart disease in the Erasmus Medical Center, Rotterdam, the Netherlands. Patients older than 18 years of age were included if they had a history of paroxysmal AF, persistent AF or longstanding persistent AF. Exclusion criteria included the presence of accessory atrioventricular pathways, previous ablative therapy or cardiac surgery, radiation therapy of the chest, atrial pacemaker leads, a left ventricular ejection fraction <30%, an estimated glomerular filtration rate <30 mL/min, and the need for inotropic or mechanical support at the time of surgery. Clinical data were collected from patient files. The study was approved by the Medical Ethical Committee (MEC 2010-054 and MEC 2014-393).

MAPPING PROCEDURE. High-resolution epicardial mapping was performed after extracorporeal circulation, before induced cardiac arrest. A bipolar electrode was temporarily connected to the high RA as a reference. A steel wire was connected to the substernal fat as an indifferent electrode. Mapping arrays contained an electrode grid of 128 electrodes (n = 13; electrode spacing: 2 millimeters; electrode diameter: 0.65 millimeters) or 192 electrodes (n = 58; electrode spacing: 2 millimeters; electrode diameter: 0.45 millimeters). During the mapping procedure, the surgeon shifted the mapping array along the epicardial surface of the RA, anterior left atrioventricular groove (LAVG), PV area, and BB, following a predefined mapping scheme.[9] Ten seconds of atrial unipolar electrocardiography together with lead I of the surface electrocardiogram were recorded at a sampling frequency of 1,000 Hz, amplified (gain: 1,000), filtered (bandwidth: 0.5-400 Hz), analogue-to-digital converted (16 bits), and stored on a hard drive. When AF was not spontaneously present on commencement of the mapping procedure, AF was induced by 10-second pacing bursts at the high RA. Extensive details of the mapping procedure have been described previously.[9]

SIGNAL PROCESSING. Customized software was used to automatically annotate local activation times, defined as the moment of the steepest negative deflection of the unipolar potential if its peak-to-peak amplitude and slope exceeded, respectively, 0.3 mV and −0.05 mV/ms. To prevent overdetection of local activation times due to fractionation of the unipolar potential, the refractory period was set at 50 ms.[10,11] In case of negative deflections within 50 milliseconds from the local activation time, the unipolar potential was labeled as fractionated. Erroneous annotations due to baseline drift, noise, artefacts or ventricular far field activity were removed manually and independently checked by 2 experienced investigators. Local activation times were used to reconstruct isochronal maps and wave trajectories in color-coded wave maps, demonstrating each individual fibrillation wave.[12] Atrial fibrillation cycle length (AFCL) was defined as time between 2 consecutive local activation times. Histograms were

ABBREVIATIONS AND ACRONYMS

AF = atrial fibrillation

AFCL = atrial fibrillation cycle length

BB = Bachmann's bundle

CFAE = complex fractionated atrial electrograms

$CFAE_{max}$ = recording site with the shortest fractionation index

DF = dominant frequency

DF_{max} = recording site with the maximum dominant frequency

LAVG = left atrioventricular groove

RA = right atrium

PV = pulmonary vein

JACC: CLINICAL ELECTROPHYSIOLOGY VOL. 9, NO. 7, 2023
JULY 2023:1082–1096

created using all AFCLs. Long AFCLs, defined as intervals exceeding 1.5 times the most frequently occurring AFCL (mode of the AFCL histogram), were manually checked for accuracy. Long AFCLs were accepted if there was: 1) an unambiguous isoelectric line separating consecutive potentials; or 2) an isolated area consisting of adjacent electrodes with long AFCLs. Long AFCLs at the borders of the mapping array were automatically excluded from analysis to avoid false-positive long AFCLs due to temporary loss of contact.

IDENTIFICATION OF $CFAE_{max}$ SITES AND DF_{max} DOMAINS. Similarly, as in previous studies, the fractionation index was calculated as mean time between all subsequent negative deflections—including all components from fractionated potentials—at each individual electrode and is a measure for the "degree" of potential fractionation at recording sites. Continuous electrical activity was defined as a fractionation index <50 milliseconds.[13] In the present study, CFAE regions consist of adjacent recording sites with a fractionation index <50 milliseconds.[13-15] $CFAE_{max}$ sites indicate the recording site with the shortest fractionation index of all recording sites.

For calculating DFs, Python's computing packages Matplotlib and Scipy were used. Voltage-time plots derived from raw electrograms were windowed with a Hann window to minimize the impact of incomplete electrograms at the beginning and end of the recordings, and were used to calculate the DF of each electrode by applying fast Fourier transformation.[16] Ventricular farfield signals were not removed before calculating DF, because ventricular component removal methodologies may introduce artifacts in the atrial electrograms and leave remnants of ventricular electrograms. However, to assess whether removing ventricular signals leads to different conclusions in our study, we recalculated the main results as obtained with ventricular farfield removal as described in the Supplemental Methods.

The frequency peak with the largest magnitude (DF) was detected in each mapping location within the range of 3.3-20.0 Hz (the equivalent of cycle lengths ranging from 300 ms to 50 ms), similarly to previous research on DFs.[17,18] When the same DF was found in multiple adjacent electrodes, these electrodes together were regarded as 1 DF domain. The inverse of Hz - corresponding to AFCL, for example 20 Hz (50 ms) were reported. Global maximum DF (DF_{max}) domains were defined as the maximum DF measured throughout both atria, and the local DF_{max} domains as the maximum DF measured within each mapping location.

ADDITIONAL CRITERIA FOR DETECTION OF SOURCE-LIKE ACTIVITY. Additional criteria applied in previous ablation studies were used to identify DF domains as targets for AF ablation. Global DF_{max} domains in those studies were defined as target sites only when: 1) the DF_{max} was higher than 8 Hz (cycle length shorter than 125 milliseconds)[7]; or 2) the global DF_{max} was also at least 20% faster than DFs at neighboring electrodes.[19] We applied these criteria to investigate whether they can indeed be used at a high-resolution scale to detect focal or rotational patterns of activation. Also, we assessed whether there is a correlation between the absolute value of fractionation index and the occurrence of source-like activity.

CHARACTERIZATION OF SPATIAL ACTIVATION PATTERNS. To quantify the occurrence of distinct patterns of activation at DF_{max} and $CFAE_{max}$ recording sites, each local activation time was assigned to a specific pattern of activation: focal activation, rotational pattern of activation, smoothly propagating fibrillation wave, fibrillation wave with interwave or intrawave conduction block (CB), collision of wavefronts, or remnant electrical activity.

In line with previous published criteria, patterns of activation required fibrillation waves propagating across at least 3 other electrodes.[12] Source-like activation was defined as a recurrent pattern of focal or reentrant activation.[20] Local activation times completely surrounded by activations later in time were regarded as the origin of a focal fibrillation wave.[12] Also, to be consistent with previous mapping studies, a time delay of at least 40 ms was required between the focal activation starting point and adjacent fibrillation waves to correct for discontinuous conduction from nearby electrodes.[12,21] Using local activation time maps, reentrant activation was defined as continuous repetitive propagation of a wavefront that returns to its origin to reactivate its pathway. Reentrant fibrillation waves were visually independently confirmed by reassessment of the activation maps by 2 investigators. Fibrillation waves were classified as smoothly propagating fibrillation waves when the conduction time (CT) toward at least 6 out of 8 adjacent electrodes was 11 milliseconds or less. To prevent overestimation of the amount of conduction block, fibrillation waves with CB contained blocking of conduction (CT >11 milliseconds) in at least 2 directions. The classification wavefront collision was assigned when 2 fibrillation waves terminated at adjacent electrodes with a CT of 2 milliseconds or less. We also observed fibrillation waves activating fewer than 4 electrodes, which were

FIGURE 1 Classification of Fibrillation Waves

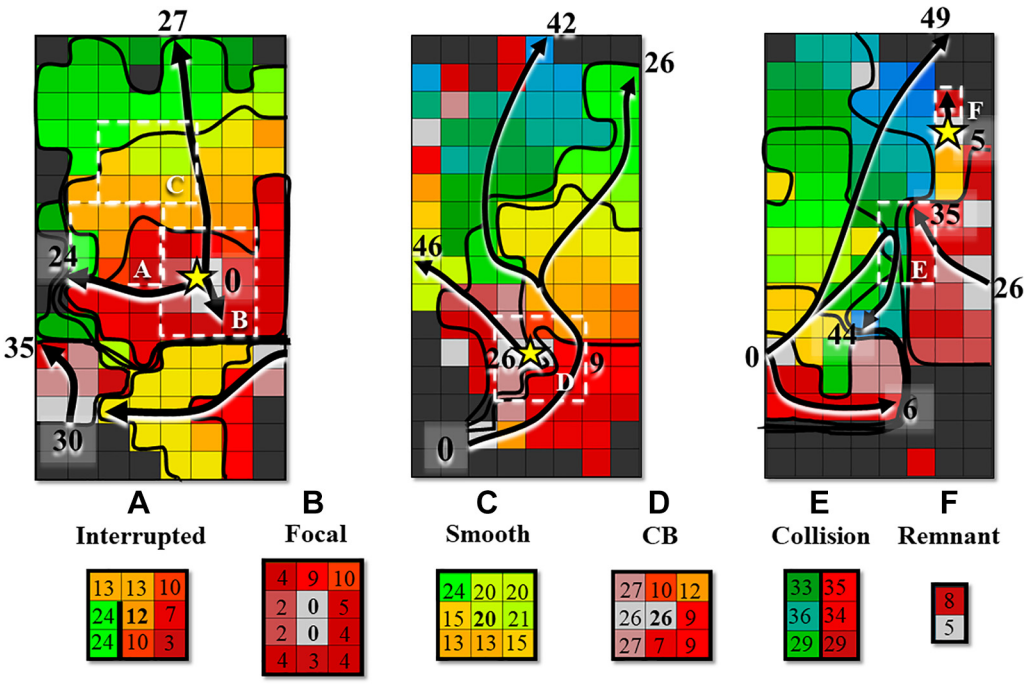

(Top) The 3 panels show local activation time maps, each reconstructed from 70 ms of atrial fibrillation (AF) derived from AF recordings in the same patient. **(Bottom)** In the highlighted boxes, an example for each prespecified category of activation patterns is provided. All recorded fibrillation waves were classified as **(A)** fibrillation waves with conduction block, **(B)** focal fibrillation waves, **(C)** smoothly propagating fibrillation waves, **(D)** fibrillation waves with conduction block (CB), **(E)** collision, or **(F)** remnant activity. Reentry of fibrillation waves was not detected and therefore not portrayed. **Black arrows** indicate the main trajectory of fibrillation waves and **thick black lines** mark lines of CB. **Yellow stars** indicate the origin of a focal fibrillation wave.

labeled as remnant activity. The upper panel of Figure 1 depicts examples of these patterns of activation in local activation time maps—each depicting 50 ms of AF- reconstructed from an AF recording from the PV area. The first local activation times map shows propagation classified as "fibrillation waves with CB" (Figure 1A), "focal pattern of activation" (Figure 1B) and "smoothly propagating fibrillation waves" (Figure 1C); the second local activation times map shows "discontinuous activation" (Figure 1D); and the third local activation times map shows "collision of fibrillation waves" (Figure 1E) and "remnant activity" that was confined to fewer than 4 electrodes (Figure 1F). There is no example of a reentry circuit, because none were detected in our study population.

ASSESSMENT OF FRACTIONATION. The degree of fractionation of unipolar fibrillation potentials was determined to assess the relation between fractionation and DF_{max} domains. Potential fractionation was classified according to the number of negative deflections into single potentials, double potentials, and fractionated potentials, containing, respectively, 1, 2 (deflections >15 milliseconds apart), and 3 or more deflections.

The proportion of fractionated potentials during 10 seconds of AF was calculated relative to the total number of potentials. In addition, regularity of the AFCL was determined by calculating the standard deviation of AFCL at each recording site.

STATISTICAL ANALYSIS. All continuous data were plotted in histograms to assess normality. Skewed continuous data were reported as median (IQR); comparison of continuous data between different subtypes of AF was performed by means of the Kruskal-Wallis test. Categoric data were expressed as absolute numbers (percentages) and compared between groups by means of chi-square or Fisher's exact test if appropriate. To determine whether there were preferential regions for DF_{max} domains and

$CFAE_{max}$ sites, chi-square tests were performed for patients in whom AF recordings of sufficient quality were obtained from at least 3 atrial regions. Equality of distribution of fractionated potentials across different atrial regions was assessed by means of Friedman's test. For each patient, potential fractionation at global DF_{max} domains or $CFAE_{max}$ sites was compared with fractionation at other recording sites by means of Wilcoxon's signed ranks test. Spearman's correlation was applied to investigate correlations between global DF_{max} domains or global $CFAE_{max}$ sites and the occurrence of specific activation patterns. In general, a 2-sided P value of <0.05 was regarded as statistically significant. Bonferroni-adjusted P values were applied to compare the occurrence of different potential subtypes ($P < 0.0167$ [ie, 0.05/3]) and various activation patterns ($P < 0.083$ [ie, 0.05/6) at DF_{max} domains and $CFAE_{max}$ sites to their occurrence at other recording sites. IBM SPSS Statistics for Windows, version 25 (IBM Corp) was used for the statistical analyses.

RESULTS

PATIENT CHARACTERISTICS. Patient characteristics are summarized in Table 1. All participants (n = 71; age 69 ± 9 years, 75% male) had a history of paroxysmal AF (n = 27), persistent AF (n = 26), or longstanding persistent AF (n = 18), and median time since AF diagnosis was 1.6 years (range: 7 days to 42 years). Forty-five patients (63%) had AF at the start of the mapping procedure; in the other patients, AF was induced by fixed rate programmed electrical stimulation. In 48 out of 69 patients (70%) the LA was dilated (LA volume index: 47 ± 24 mL/m^2); in 5 patients, LA dimensions could not be collected from patient files.

MAPPING CHARACTERISTICS. In the entire study population, 1,350 (IQR: 1,075-1514) recording sites were analyzed per patient. Owing to low signal-to-noise ratio or artifacts, 15% ± 8% of recording sites per patient were excluded. Median AFCLs at the RA, BB, LAVG, and PV were, respectively, 170 milliseconds (range 153-188 milliseconds), 164 milliseconds (145-179 milliseconds), 156 milliseconds (142-179 milliseconds), and 155,milliseconds (143-175 milliseconds).

SPATIAL DISTRIBUTION OF DF_{max} AND $CFAE_{max}$. Bar charts in Figure 2 show the location of global DF_{max} domains and $CFAE_{max}$ sites found in the entire study population. The global DF_{max} domain was most frequently located along the LAVG (RA 32%, BB 3%, LAVG 60%; PV 17%; $P = 0.002$), whereas the PV area was predominant for $CFAE_{max}$ sites (RA 11%, BB 29%, LAVG 16%; PV 44%; $P < 0.001$). Median AFCLs did not differ between global DF_{max} domains and other recording sites (162 milliseconds [IQR: 141-187 milliseconds] vs 157 milliseconds [146-178 milliseconds]; $P = 0.68$), but AFCL regularity was higher (SD of AFCL: 20 milliseconds [12-33 milliseconds] vs 37 milliseconds [32-46 milliseconds]; $P < 0.001$).

The atrial surface area covered by global DF_{max} domains varied considerably between patients, ranging from 1 to 117 electrodes (median: 2), covering 0.05% to 5.74% (median: 0.12%) of the total area

TABLE 1 Patient Characteristics (N = 71)

Age, y	69 ± 9
Female	18 (25)
Risk factors	
BMI, kg/m^2	28 ± 5
Diabetes mellitus	19/70 (27)
Hypertension	43/70 (61)
Underlying heart disease	
IHD	7 (10)
VHD	45 (63)
VHD + IHD	9 (13)
CHD	10 (14)
History of myocardial infarction	9 (13)
AF subtype	
Paroxysmal	28 (39)
Persistent	26 (36)
Longstanding persistent	17 (23)
Time since AF diagnosis, y	1.64 (0.59-7.13)
LA enlargement	
Not dilated	23/67 (34)
Mildly dilated	8/67 (12)
Moderately dilated	6/67 (9)
Severely dilated	30/67 (45)
LAVI, mL/m^2	47 ± 24
LV function	
Normal	54 (76)
Mild impairment	15 (21)
Moderate impairment	2 (3)
Antiarrhythmic drugs	
Class I	2 (3)
Class II	48 (68)
Class III	7 (10)
Class IV	1 (1)
Digoxin	13 (18)
Procedural characteristics	
AF at start of procedure	46 (65)
Mapping array	
192 electrodes	58 (82)
128 electrodes	13 (18)

Values are mean ± SD, n (%), or median (IQR).

AF = atrial fibrillation; AVD = aortic valve disease; BMI = body mass index; CHD = congenital heart disease; IHD = ischemic heart disease; LA = left atrium; LAVI = left atrial volume index; LV = left ventricular; VHD = valvular heart disease.

FIGURE 2 **Spatial Distribution of $CFAE_{max}$ and DF_{max}**

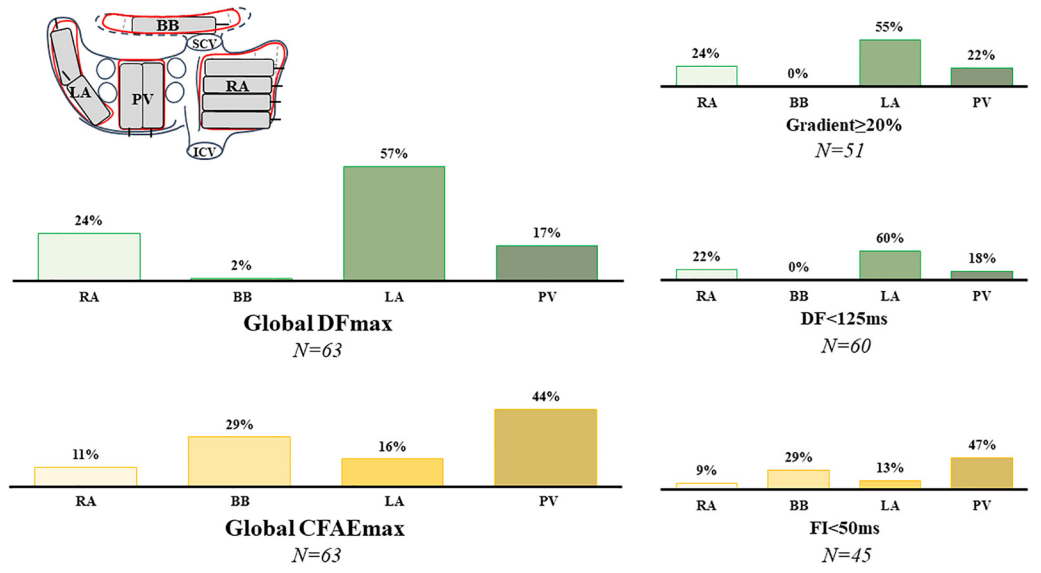

Bar charts showing the location of global DF_{max} domains and $CFAE_{max}$ sites found in the entire study population, with **(left)** and without **(right)** additional criteria to define high-frequency sites. $CFAE_{max}$ = site with shortest fractionation index; BB = Bachmann's bundle; DF = dominant frequency; DF_{max} = maximum dominant frequency; FI = fractionation index; LA = left atrioventricular groove; PV = pulmonary vein area; RA = right atrium.

mapped. All global $CFAE_{max}$ sites covered only 1 (n = 69) or 2 electrodes (n = 2). CFAE regions (fractionation index <50 ms) were present in 47 patients (66%) and covered 20 (IQR: 8-79) electrodes (or 0.06% [IQR: 0.04%-0.21%] of all recording electrodes). In only 5 patients (7%), the global DF_{max} domain and $CFAE_{max}$ site were both located in the same mapping location; the shortest distances from each $CFAE_{max}$ site to the perimeter of the DF_{max} domain were 0, 3, 4, 9, and 24 millimeters.

In 2 out of 64 patients (3%), the DF_{max} domain, when calculated with QRS subtraction, was closely located to the recording site with the highest proportion of focal fibrillation waves. In one of these patients, however, other recording sites harbored the same proportion of focal fibrillation waves, but the DFs were not affected. In the other patient, the focal pattern of activation was present in a relatively small proportion of the entire recording period (23%). It remains questionable whether such a low proportion of focal waves can be regarded as a driver of the AF process (see the Supplemental Results section for more detail on this separate analysis).

PATTERNS OF ACTIVATION AT DF_{max} AND $CFAE_{max}$. Patterns of activation identified at all global DF_{max} domains and $CFAE_{max}$ sites are summarized in Supplemental Tables 1 and 2. At global DF_{max} domains, fibrillation waves were rarely focal fibrillation waves (0.0% [IQR: 0.0%-1.5%]); focal waves did not occur more frequently at these domains than at other recording sites in the atria of the same patient (0.6% [IQR: 0.5%-0.7%]; $P = 0.78$). Smoothly propagating fibrillation waves, however, had a higher incidence (at global DF_{max} domains: 22% [IQR: 7%-48%]; at other recording sites: 17% [IQR: 11%-24%]; $P = 0.001$ [$P < 0.083$]), whereas fibrillation waves with CB occurred less frequently (69% [IQR: 51%-81%] vs 74% [IQR: 69%-78%]; $P = 0.006$). Wavefront collision occurred rarely (global DF_{max} domains: 0.0% [IQR: 0.0%-0.0%]; other recording sites: 0.10% [IQR: 0.07%-0.14%]; $P < 0.001$). 2% [IQR: 1%-8%] of fibrillation waves at DF_{max} domains (other recording sites: 8% [IQR: 5%-10%]; $P = 0.001$) were classified as remnant activity.

At $CFAE_{max}$ sites, 20% [IQR: 12%-29%] of all waves were classified as remnant activity; which was less frequently observed at other recording sites (8% [IQR: 5%-10%] of fibrillation waves; $P < 0.001$). Patterns of activation detected at $CFAE_{max}$ sites were less frequently smoothly propagating waves (1% [IQR: 0%-1%] vs 17% [IQR: 12%-24%]; $P < 0.001$) or

FIGURE 3 Relationship Between Focal Activation Patterns and Methods of Source Detection

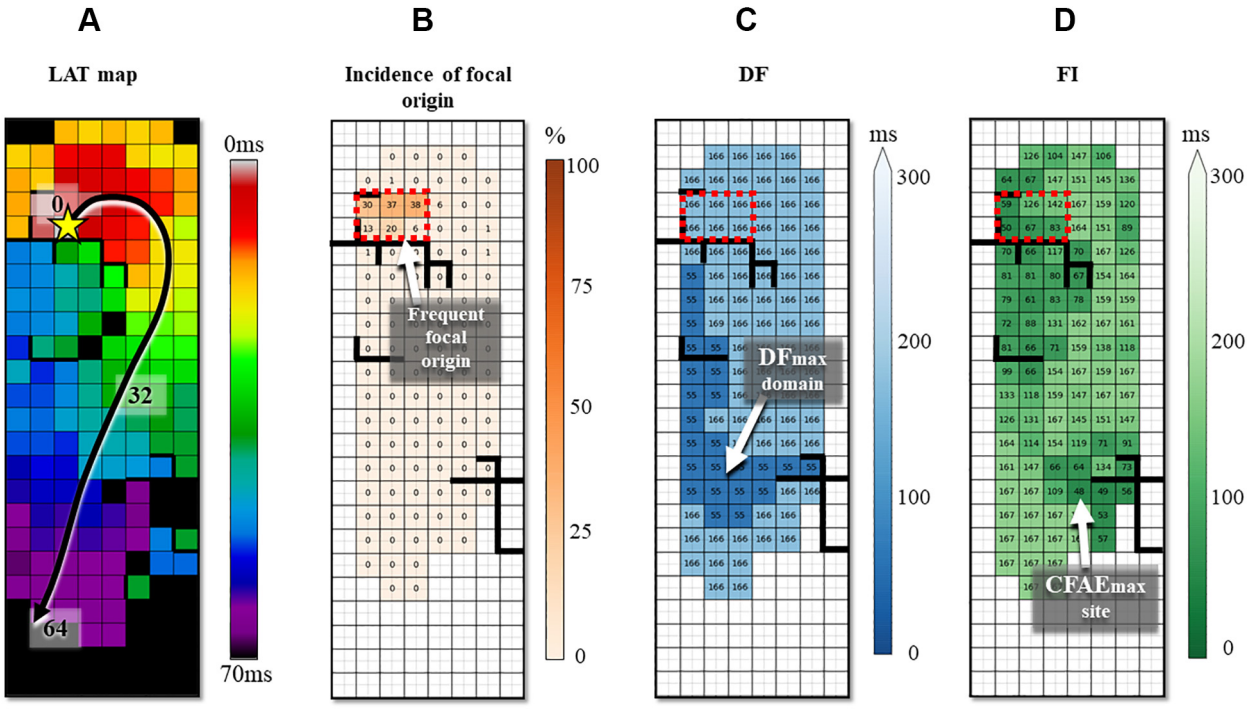

(A) Local activation times map, derived from the left atrial (LA) appendage of a patient with persistent atrial fibrillation (AF), showing a focal pattern of activation (origin indicated by yellow star), propagating around a line of conduction block to excite the entire mapping location. For the same mapping location, other panels summarize per electrode the proportion of focal activation **(B)**, and the corresponding local DF **(C)** and FI. Although the origin of focal fibrillation waves frequently occurs in the same confined area demonstrated in **A** (indicated by the **dotted boxed areas**), DF_{max} **(dark blue)** and $CFAE_{max}$ **(dark green)** are found at other recording sites. In the majority of other patients, detected patterns of focal activation were less repetitive. The **black arrow** indicates the main trajectory of the fibrillation wave. **Thick black lines** indicate lines of conduction block. **Yellow star** indicates the origin of a focal fibrillation wave. BB = Bachmann's bundle; $CFAE_{max}$ = site with shortest fractionation index; DF = dominant frequency; DF_{max}: maximum dominant frequency; FI = fractionation index; LAVG = left atrioventricular groove; PV = pulmonary vein area; RA = right atrium.

wavefront collision (0.0% [IQR: 0.0%-0.0%] vs 0.11% [IQR: 0.07%-0.14%]; $P < 0.001$). Remarkably, there was no difference in the occurrence of fibrillation waves with CB (74% [IQR: 67%-84%] vs 74% [IQR: 68%-78%]; $P = 0.311$) or focal fibrillation waves ($CFAE_{max}$: 1.0% [IQR: 0.0%-2.3%]; other recording sites: 0.6% [IQR: 0.5%-0.8%]; $P = 0.182$ [$P > 0.083$]).

Interestingly, reentry of fibrillation waves was not observed at any of the DF_{max} domains and $CFAE_{max}$ sites.

RELATIONS BETWEEN DF_{max} OR $CFAE_{max}$ AND FOCAL PATTERNS OF ACTIVATION. In all 71 patients, focal patterns of activation occurring repetitively during at least 20% of the recording was observed in 11 patients (15%). Remarkably, even in these cases of repetitive focal activation, there was no relationship between DF_{max} and origins of focal fibrillation waves. The local activation times map in Figure 3A shows the occurrence of a focal fibrillation wave at the LA appendage in the upper part of the mapping area. This pattern of activation occurred repetitively (59 times) during 10 seconds of AF (Video 1). The recording site at which the focal fibrillation waves occurred most frequently (red boxed area in Figure 3B) did not correspond to the location of local DF_{max} (arrow in Figure 3C) or $CFAE_{max}$ (arrow in Figure 3D). Continuous electrical activity at the $CFAE_{max}$ site was caused by fibrillation waves repetitively propagating around a line of CB (thick black line), as illustrated by 10 seconds of consecutive fibrillation local activation times maps in Video 1.

Videos 2 to 5 (corresponding to Supplemental Figures 1 to 4) show 10 seconds of consecutive fibrillation local activation times maps during AF derived from various mapping locations obtained from 4 different patients. They illustrate a poor relationship

FIGURE 4 **Correlations Between Patterns of Activation and DF_{max}/$CFAE_{max}$**

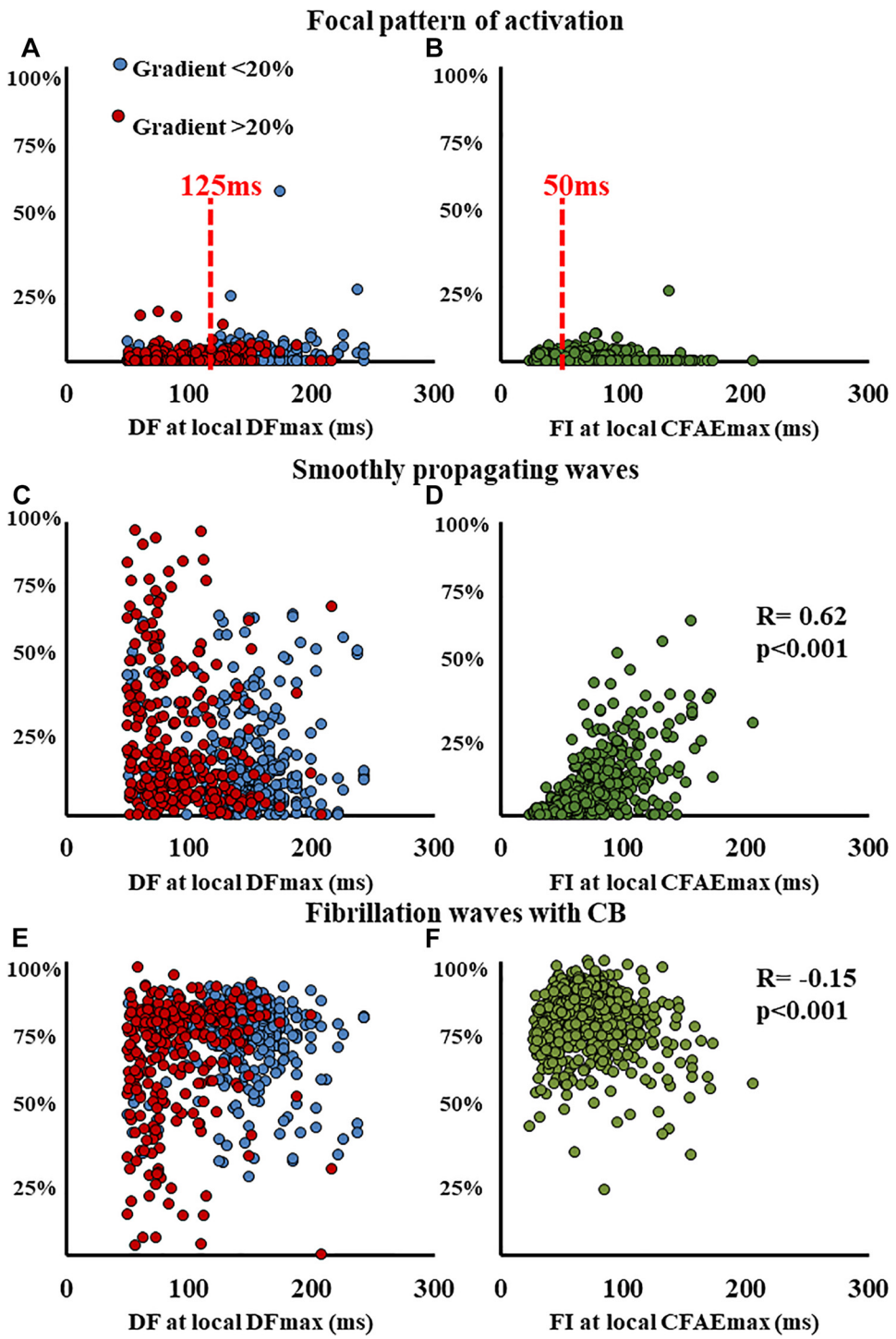

Scatterplots depict the relation between the characteristics of DF_{max} domains **(Left)** or $CFAE_{max}$ sites **(Right)** and the corresponding incidence of focal patterns of activation. There was no relation between focal patterns of activation and local DF_{max} domains **(A)** or the fractionation index **(B)**. Cut-off values of 8Hz (125 ms) for DF_{max} domains and 50ms for $CFAE_{max}$ sites and the presence of frequency gradient of ≥20% for DF_{max} domains (indicated by red markers) did not improve source identification. There were no relations between local DF_{max} and the incidence of smoothly propagating waves **(C)** or fibrillation waves with CB **(E)**. Local $CFAE_{max}$ were weakly correlated to the incidence of smoothly propagating waves **(D,** rho: 0.62, $P < 0.001$) and fibrillation waves with CB **(F,** rho: -0.15, $P < 0.001$). $CFAE_{max}$ = recording site with shortest fractionation index; DF = dominant frequency, DF_{max} = maximum dominant frequency; FI = fractionation index.

JACC: CLINICAL ELECTROPHYSIOLOGY VOL. 9, NO. 7, 2023
JULY 2023:1082–1096

among DF_{max} domains, $CFAE_{max}$ sites, and the occurrence of focal fibrillation waves.

VALUE OF ADDITIONAL CRITERIA TO ENHANCE SOURCE DETECTION WITH THE USE OF DF_{max}. In 67 patients (94%), at least 1 local DF_{max} domain with a DF >8 Hz (cycle length <125 milliseconds) was present (median: 4; range: 1-11 milliseconds). In 65 patients, a median of 4 (range: 2-6) local DF_{max} domains with a frequency gradient >20% were detected. The relationship between characteristics of these DF_{max} domains and corresponding incidence of focal fibrillation waves is depicted in a scatterplot in **Figure 4**, showing that there is no relation between the occurrence of focal fibrillation waves and DF >8 Hz (<125 milliseconds) or local DF_{max} domains with a frequency gradient >20%. There was also no linear relation between DF or DF_{max} >20% and the incidence of smoothly propagating fibrillation waves or fibrillation waves with CB (**Figure 4**).

VALUE OF ADDITIONAL CRITERIA TO ENHANCE SOURCE DETECTION USING $CFAE_{max}$. In previous studies, continuous CFAE regions (fractionation index <50 milliseconds) were assumed to be related to continuous electrical activity[13] and therefore regarded as a possible marker for reentry of fibrillation waves or adjacency to focal sources. We therefore assessed whether an increased amount of fractionation (a lower fractionation index) indeed correlates to more frequently occurring focal patterns of activation. However, as shown in **Figure 4**, there was no correlation between fractionation index at recording sites and the occurrence of focal fibrillation waves (Pearson's rho = −0.018; $P < 0.643$) and only weak or moderate correlations between fractionation index and fibrillation waves with CB (rho = −0.15; $P < 0.001$) or smooth propagation of fibrillation waves (rho = 0.62; $P < 0.001$) were detected.

POTENTIAL MORPHOLOGY AT DF_{max} AND $CFAE_{max}$ SITES. As summarized in bar charts in **Figure 5**, single potentials were most often recorded throughout all recording sites, the median proportion ranging from 58% to 63% ($P < 0.001$ for each region). Fractionated potentials were recorded from all regions in all patients. However, single potentials occurred most frequently at the LAVG and at BB, whereas the proportion of fractionated potentials was highest at the PV and RA (single potentials: $P = 0.018$; fractionated potentials: $P < 0.001$).

The occurrence of fractionated potentials at primary DF_{max} domains and $CFAE_{max}$ sites was compared to the occurrence of fractionated potentials at all other recording sites as summarized in Supplemental Table 3. As depicted in **Figure 5**, global DF_{max} electrograms contained a larger proportion of single potentials (72% [IQR: 55%-84%] vs 61% [IQR: 55%-65%]; $P = 0.003$) and a lower number of double potentials (4% [IQR: 1%-11%] vs 12% [IQR: 11%-14%]; $P < 0.001$) and fractionated potentials (4% [IQR: 1%-11%] vs 12% [IQR: 9%-15%]; $P = 0.004$). The electrograms at 4 DF_{max} domains from randomly selected patients are depicted in **Figure 6**. They illustrate the high proportion of single potentials and relative regularity of AFCLs frequently found at DF_{max} domains.

Electrogram fractionation at global $CFAE_{max}$ sites was also compared to fractionation at other recording sites, as summarized in Supplemental Table 4. Electrograms at global $CFAE_{max}$ sites contain a smaller proportion of single potentials (21% [IQR: 15%-30%] vs 61% [IQR: 55%-65%]; $P < 0.001$) and more fractionated potentials (52% [IQR: 43%-66%] vs 12% [IQR: 9%-14%]; $P < 0.001$) than at other recording sites. Examples of electrograms recorded at $CFAE_{max}$ sites are shown in **Figure 7**, and are derived from the same patients as depicted in **Figure 6**. Recording sites at $CFAE_{max}$ are typically fractionated and show high AFCL irregularity.

INCIDENCE OF FOCAL FIBRILLATION WAVES. In each patient, the areas with the highest proportion of focal fibrillation waves were localized to identify possible AF sources. The maximal proportion of focal fibrillation waves recorded ranged from 8% to 89% (median: 19%) and was most frequently located at the RA or LAVG (RA 49%, LAVG 44%, BB 16%, PV 10%; $P = 0.001$). This corresponded to a median of 10 focal fibrillation waves (range: 3-50) occurring at the same recording site for 10 seconds, although they were not always consecutive. The median total number of fibrillation waves at the same recording sites was 60 (range: 51-71) In 4 patients, the highest proportion of focal fibrillation waves was greater than 50%; of which all 4 focal wave origins were found at the LA appendage. DF_{max} domains were not identified at the focal wave origin. Median AFCL at sites of maximum repetition was 156 milliseconds and ranged from 86 milliseconds to 245 milliseconds, which was not shorter than the median AFCL at other recording sites within the same patient (155 milliseconds [IQR: 110-243 milliseconds]; uncorrected $P = 0.042$). AFCL at sites of maximum repetition was more regular than at other recording sites (SD: 27 milliseconds [range: 7-67 milliseconds] vs 36 milliseconds [14-57 milliseconds]; $P < 0.001$).

The degree of potential fractionation at recording sites where focal fibrillation waves emerged most

frequently were not different from unipolar electrocardiograms at other recording sites.

DISCUSSION

In this study, we used epicardial mapping to characterize patterns of activation underlying DF_{max} domains and $CFAE_{max}$ sites at a high-resolution scale in the majority of the atria, including BB, in patients with different subtypes of AF. Although DF_{max} domains and $CFAE_{max}$ sites were detected in all patients, they were not related to focal fibrillation waves or rotational activation indicating driving sources of AF. We demonstrated that using additional, more specific criteria to define target sites—including the presence of a DF >8 Hz (cycle length <125 milliseconds), DF gradient >20%, or fractionation index <50 milliseconds, as previously applied in clinical studies—also did not result in source identification. The pattern of activation occurring most frequently at $CFAE_{max}$ sites consisted of fibrillation waves encountering areas of CB and remnant activity, which in turn corresponded to a predominance of fractionated potentials. Surprisingly, mainly smoothly propagating waves gave rise to DF_{max} domains, and electrograms recorded at these sites consisted mostly of single potentials and double potentials. Findings of the present study do not support the concept of DF_{max} domains or $CFAE_{max}$ sites as target sites for ablation of AF.

IMPACT OF PATTERNS OF ACTIVATION ON DF_{max} AND $CFAE_{max}$. In all patients, DF_{max} domains or $CFAE_{max}$ sites were detected that would have qualified as ablation targets for AF according to criteria applied in previous clinical studies. However, we found that both DF_{max} domains and $CFAE_{max}$ sites did not correspond to the origin of repetitive focal fibrillation waves or rotational activity.

At recording sites of DF_{max} domains, smoothly propagating fibrillation waves were observed more often than at other recording sites. Similar observations were made in the sheep model by Skanes et al[22] (bipolar epicardial electrogram and high-density optical recording of the LA and RA). In that sheep model of AF, fibrillation waves at DF_{max} domains most frequently emerged from the border of the array. The authors proposed that the origins of the sources were located beyond the mapped region. However, our observations do not support that explanation. In our data, 32 out of 61 DF_{max} domains (~50%) were embedded within the middle of the mapping area and thus surrounded by recording sites with lower DFs but did not correspond to the origin of source-like activation patterns.

As an alternative to source-like activity, it was also proposed that high-DF sites may be derived from the fractionated potentials occurring around wavefront collision sites or lines of conduction block.[19] In contrast, we found that lines of CB occurred less frequently at DF_{max} domains than at other recording sites. Especially when the array was activated by

FIGURE 5 Distribution of Potential Fractionation

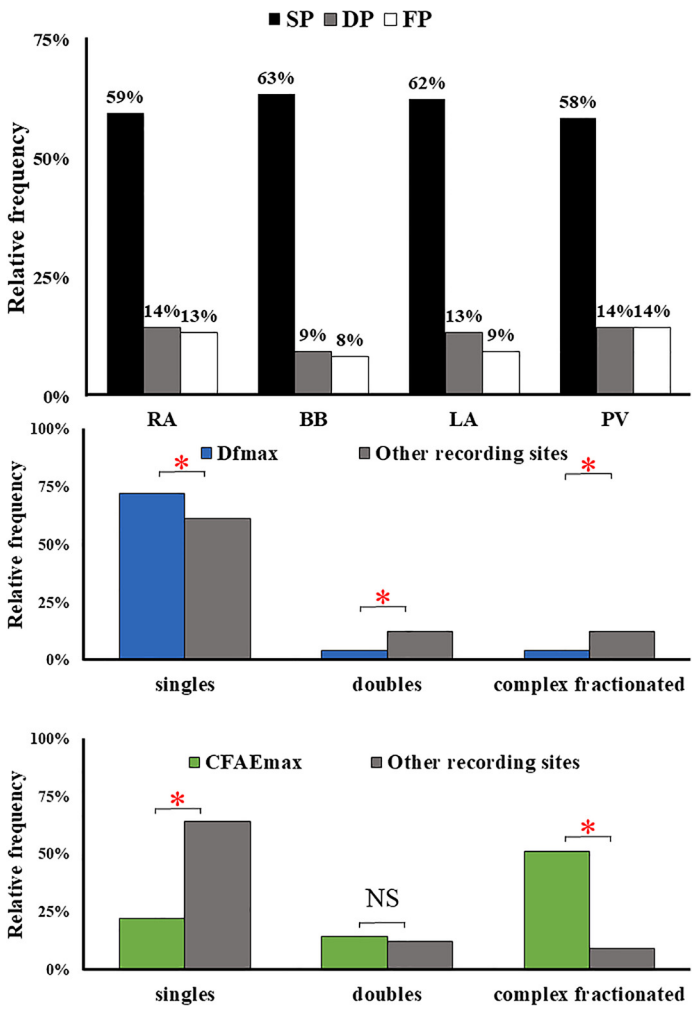

(Top) Bar charts summarize the relative frequency distribution of single (SP), double (DP), and fractionated (FP) potentials throughout the atria in the entire patient population. SPs occur the most frequently in each mapping region ($P < 0.001$). **(Middle)** Bar charts compare the occurrence of potential subtypes at DF_{max} domains with their occurrence at all other recording sites. **(Bottom)** Bar charts compare the occurrence of potential subtypes at $CFAE_{max}$ sites with their occurrence at all other recording sites. **Asterisks** indicate statistical significance based on Bonferroni-corrected *P* values (threshold for significance: $P < 0.0125$). Abbreviations as in Figure 3.

FIGURE 6 Electrograms at DF_{max} Domains

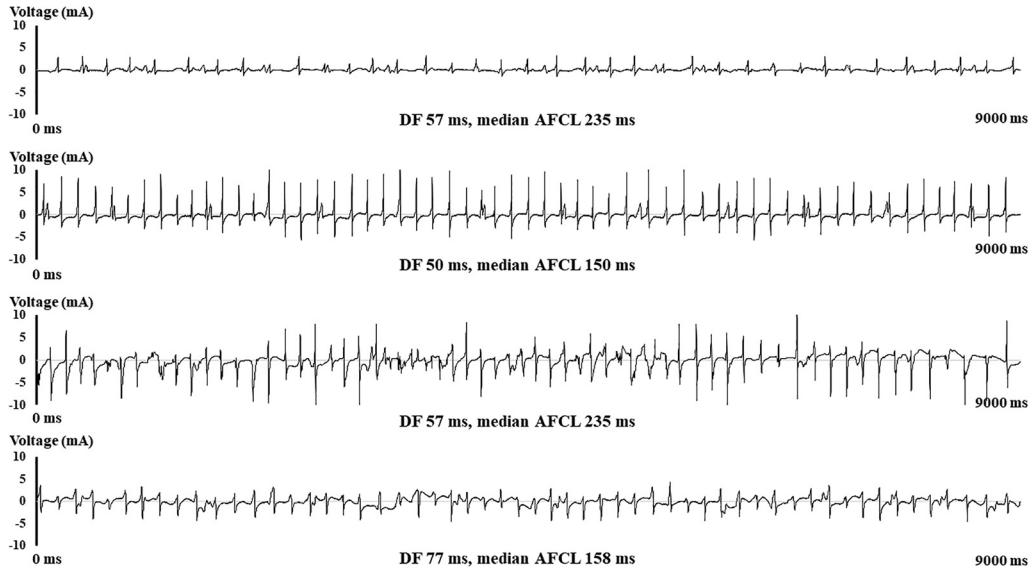

Electrograms recorded at DF_{max} domains of 4 different patients reflect typical electrograms found in these regions, showing a high proportion of single potentials. In the second example, the DF (50 milliseconds) is 3 times shorter than the median atrial fibrillation cycle length (AFCL; 150 milliseconds). The electrograms show relatively regular single potentials without a clear explanation for erroneous DF calculation except the ventricular far field components. When these components are removed before fast Fourier transform, the DF calculated is indeed closer to the median AFCL (147 milliseconds). However, when ventricular components are removed before analysis in all electrograms of the entire study, as described in Supplemental Methods, this alteration of the methodology does not improve the detection of source-like activation at DF_{max} domains. Abbreviations as in **Figure 3**.

smoothly propagating fibrillation waves with relatively regular intervals, DF_{max} domains within these waves consisted of small areas from which single potentials and double potentials were recorded.

In previous studies, the rationale for targeting CFAEs was based on the association between CFAEs and either pivot points occurring at reentrant circuits, conduction delay,[1] or fibrillatory conduction occurring at the periphery of organized sources owing to interaction with anatomic and functional obstacles.[6,23] For example, Atienza et al[14] found that activity at variable CFAE sites at the LA included 71% functional CB resulting in reentry and 29% breakthrough waves with a line of CB. At continuous CFAE sites, Jadidi et al[15] found 71% wave collision and 24% slowed conduction as the cause of continuous CFAEs (fractionation index <80 ms). However, in both studies, low-spatial-resolution 20-polar catheters were used for AF recording. In our high-density mapping study, $CFAE_{max}$ sites were indeed frequently associated with areas of CB, but reentry of fibrillation waves was not observed, and a spatial relationship of CFAEs to DF_{max} domains was not demonstrated. Our results, therefore, do not provide a rationale for targeting CFAEs according to the existing criteria used in clinical practice to guide AF ablation. This is in line with the outcome of a large randomized controlled trial where Verma et al[2] found no additional benefit from CFAE ablation alongside PV isolation.

Throughout the years, mechanisms underlying AF initiation and persistence have been heavily debated. Theories include both organized mechanisms for AF maintenance, such as ectopic foci,[24] leading circle reentry,[25] and intramural microreentry (eg, scroll waves),[26] and disorganized mechanisms such as random wavelet reentry[27] and epiendocardial asynchrony.[12,21] However, approaches to prove any of these hypotheses are largely based on tracking similar electrophysiologic phenomena such as focal or rotational patterns of activation acting as a driver of AF. Although extensive mapping of the epicardium was

FIGURE 7 Electrograms at $CFAE_{max}$ Sites

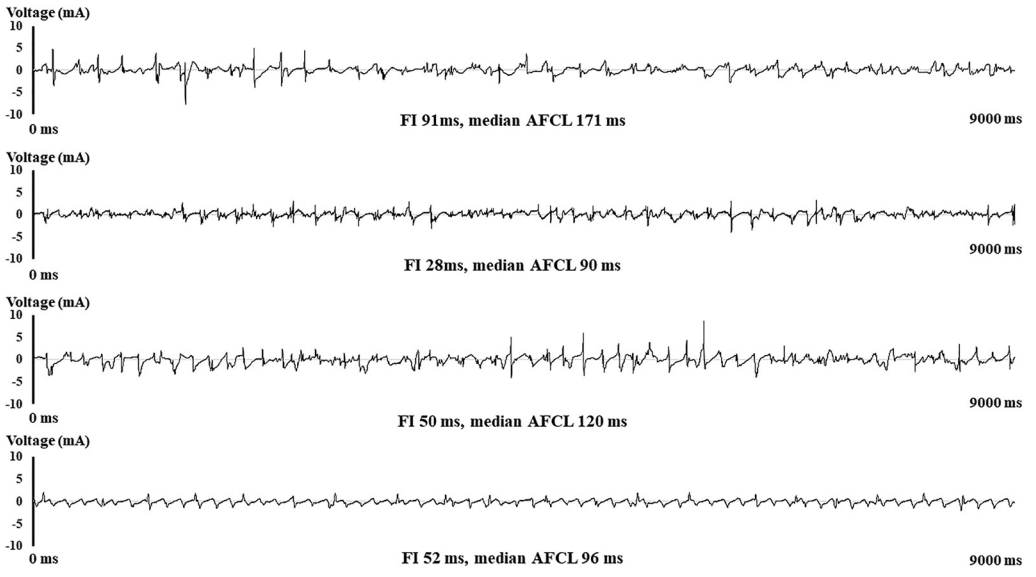

Typical electrograms recorded at $CFAE_{max}$ sites of 4 different patients. They were derived from the same patients as in Figure 6.

performed in the present study, the existence of fixed focal sources could not be proven by targeting DF_{max} domains or $CFAE_{max}$ sites.

In this study, mapping of different atrial regions occurred sequentially and not simultaneously. We could therefore detect the occurrence of focal or rotational patterns of activation in 1 mapping location but not the full length of their wave paths. Nonetheless, even in sequential mapping, the absence of repetitive source-like activation at the highest activation frequencies at any of the 93,240 recording sites contradicts a dominant role for fixed drivers in maintaining AF. In previous studies, the varying incidence of focal activation patterns combined with previously reported small R waves in the potentials recorded at the origin of focal waves and coupling intervals longer than the median AFCL[21] appeared more consistent with transmural conduction of focal fibrillation waves. Also, source-like patterns of activation in other clinical epicardial mapping studies were either not detected[12,21] or were transient.[28,29] Previous studies in which relationships between AF persistence and organized sources were found used different mapping techniques, such as global endocardial mapping with basket catheters and noninvasive body surface mapping.[20,30] Clearly, there are methodologic differences between the mapping techniques regarding spatial resolution, filtering, and data interpolation, which may explain the lack of agreement between study outcomes.

However, because the present study was focused on the use of high-frequency sites to detect source-like activation rather than unraveling mechanisms underlying AF, it does not prove the general absence of drivers during AF. We cannot completely exclude the existence of sources located in atrial regions inaccessible during epicardial mapping, such as the intra-atrial septum, although the most frequently reported location of organized sources—LA appendix or wall and PV area[22,31,32]—were covered in our mapping scheme.

RELATIONSHIP BETWEEN FRACTIONATION AND DF_{max}. To the best of our knowledge, this is the first study in which an elaborate characterization of potential morphology derived from DF_{max} domains and $CFAE_{max}$ sites is performed. As expected, electrograms at $CFAE_{max}$ sites consisted mainly of fractionated potentials (median amount: 51%). Because fractionation of electrograms is often provided as an explanation for detecting increased DF, it was surprising that the proportion of fractionated potentials at DF_{max} domains was very small (median amount: 1%). Instead, potentials

CENTRAL ILLUSTRATION **High DFs and Fractionated Potentials Do Not Indicate Focal or Rotational Activation During AF**

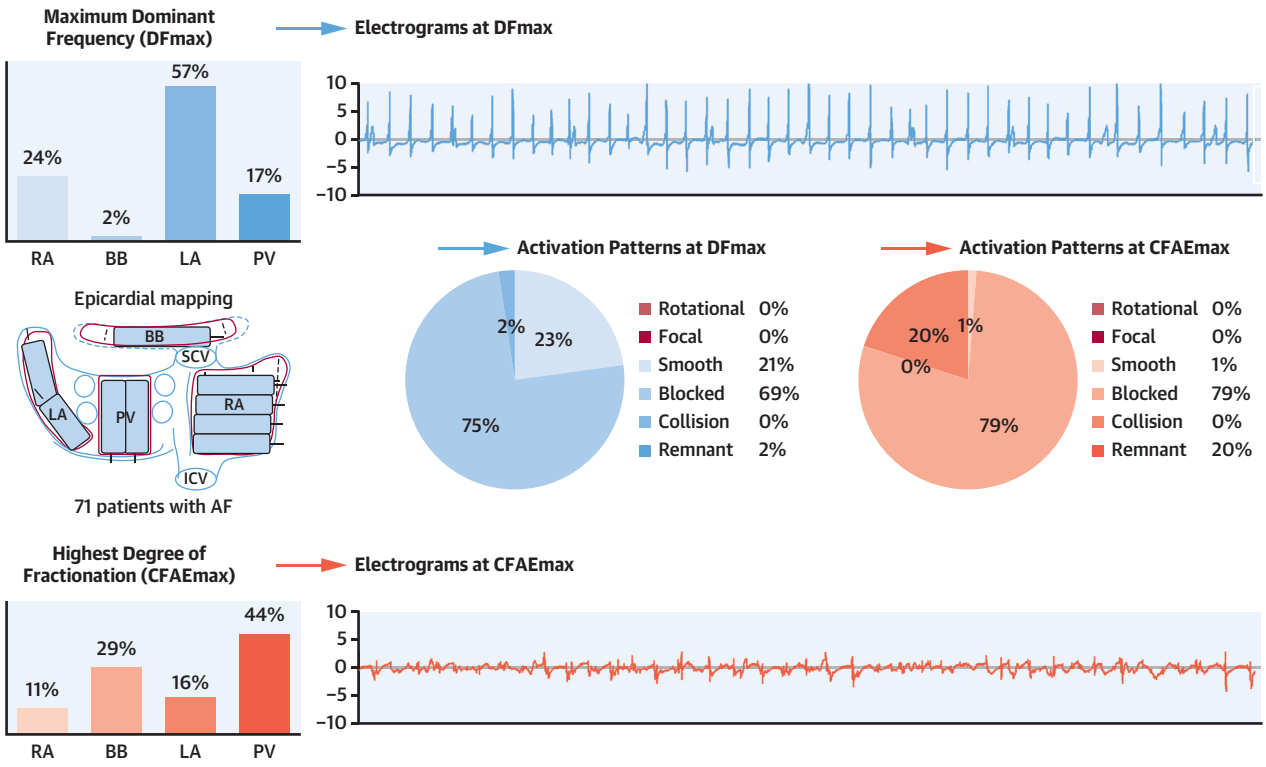

van Staveren LN, et al. J Am Coll Cardiol EP. 2023;9(7):1082-1096.

AF = atrial fibrillation; BB = Bachmann's bundle; $CFAE_{max}$ = site with shortest fractionation index; DF = dominant frequency; DF_{max} = maximum dominant frequency; LA = left atrioventricular groove; PV = pulmonary vein area; RA = right atrium.

were mainly a combination of single potentials and double potentials.

Although the DF is correlated with the inverse of the mean cycle length in case of regular beat-to-beat intervals,[33,34] this correlation is disturbed in electrograms with either fractionated potentials or increased cycle length irregularity.[35,36] Ng et al[37] demonstrated that the presence of double potentials in electrograms recorded during atrial flutter doubled the DF as double potentials increased the power of one of the harmonics (multiplications of the DF) in the frequency spectrum. An increased delay between the components of the double potentials further increased the chance of a harmonic peak becoming the DF.[37] CL irregularity especially resulted in a dispersion in frequency peaks and inaccurate DF selection. Therefore, the presence of irregular AFCLs and fractionated potentials—both of which are typically present during AF—cause an unreliable estimation of the mean activation rate. In our mapping data, the (combined) presence of single potentials and double potentials most consistently increased the DF.

STUDY LIMITATIONS. As discussed above, our mapping data was obtained sequentially from the different mapping locations. Despite excluding electrograms with inadequate signal-to-noise ratios, in some patients activation time maps revealed large simultaneously activated atrial regions, where patterns of activation could not be determined. Possibly, only remote electrical activity was recorded in these areas owing to electrical silence, the presence of epicardial fat, or inadequate array-tissue contact.[38] The arrhythmogenic substrate of our patient group does not necessarily represent the AF substrate in all patients. However, the presence of focal and reentrant activation at the LA and RA driving AF was also reported in patients with permanent AF undergoing surgical correction for mitral valve disease, suggesting that patients with and without valvular heart

disease at least partly share AF substrate characteristics.[39] In the present study, we did not investigate differences between epicardial and endocardial recordings, but in a previous study we demonstrated that despite the presence of areas of asynchronous activation, the patterns of activation (eg, areas of conduction block and focal epicardial breakthrough) waves occurring within a specific time period are similar.[23] Therefore, our findings on epicardial patterns of activation are also translatable to the endocardium. We did not perform repeated mapping to investigate stability of DF_{max} and $CFAE_{max}$ over time, to avoid excessive prolongation of cardiopulmonary bypass time.

CONCLUSIONS

In this study, we used epicardial mapping to characterize patterns of activation underlying DF_{max} domains and $CFAE_{max}$ sites at a high-resolution scale in the atria, including BB, in a large population of patients with different subtypes of AF (**Central Illustration**). DF_{max} domains and $CFAE_{max}$ sites derived from high-density epicardial electrograms do not correspond to the origin of source-like patterns of activation during AF. At DF_{max} domains, smoothly propagating fibrillation waves were especially observed, whereas $CFAE_{max}$ sites strongly correlated with the occurrence of remnant activity. Additional criteria as used in several clinical studies to improve the selection of target sites for ablation did not result in a higher detection rate for source-like patterns of activation. Our results do not support the concept of DF_{max} domains or $CFAE_{max}$ sites as target sites for ablation of AF.

ACKNOWLEDGMENTS The authors thank J.A. Bekkers, MD, PhD, C. Kik, MD: W.J. van Leeuwen, MD, F.B.S. Oei, MD, PhD, P.C. van de Woestijne, MD, F.R.N. van Schaagen, MD, A. Yaksh, MD, PhD, C.P. Teuwen, MD, PhD, E.A.H. Lanters, MD, PhD, E.M.J.P. Mouws, MD, PhD, J.M.E. van der Does, MD, PhD, R. Starreveld, MSc, PhD, C.S. Serban, DVM, A. Heida, MD, W.F.B. van der Does, MD, C. Houck, MD, PhD, R.K. Kharbanda, MD, M.C. Roos-Serote, PhD, P. Knops, M. van Schie, MSc, and A. Muskens for their contributions to this work.

FUNDING SUPPORT AND AUTHOR DISCLOSURES

Prof Dr de Groot is supported by grants from the Investigator-Initiated Study Program of Biosense Webster (IIS-331 Phase 2), CVON (grant no. 914728), NWO-Vidi (grant no. 91717339), and Medical Delta. All other authors have reported that they have no relationships relevant to the contents of this paper to disclose.

ADDRESS FOR CORRESPONDENCE: Prof Dr Natasja M.S de Groot, Unit Translational Electrophysiology, Department of Cardiology, Erasmus Medical Center, Dr Molewaterplein 40, 3015 GD Rotterdam, the Netherlands. E-mail: n.m.s.degroot@erasmusmc.nl.

PERSPECTIVES

COMPETENCY IN MEDICAL KNOWLEDGE: It is generally considered that high dominant frequencies in electrograms are translatable to high atrial activation rates caused by "drivers" of the fibrillatory process, despite the known challenges of the methodology such as beat-to-beat cycle length irregularity, fractionated potentials, and low signal-to-noise ratios. This study demonstrates that even during elaborate high-density mapping of the atria, patterns of activation detected at recording sites with the highest dominant frequencies do not confirm the presence of source-like activity.

TRANSLATIONAL OUTLOOK: To improve treatment strategies for patients with AF, it is crucial to understand the underlying mechanisms that cause and perpetuate AF. The results of this study do not support the currently applied methodologies to identifying target sites during ablation of AF. Important next steps would be to identify the substrate responsible for initiating and maintaining AF in high-density mapping, and then to determine unique characteristics of electrograms recorded at these sites.

REFERENCES

1. Nademanee K, McKenzie J, Kosar E, et al. A new approach for catheter ablation of atrial fibrillation: mapping of the electrophysiologic substrate. *J Am Coll Cardiol*. 2004;43(11):2044–2053.

2. Verma A, Jiang CY, Betts TR, et al. Approaches to catheter ablation for persistent atrial fibrillation. *N Engl J Med*. 2015;372(19):1812–1822.

3. Sohal M, Choudhury R, Taghji P, et al. Is mapping of complex fractionated electrograms obsolete? *Arrhythm Electrophysiol Rev*. 2015;4(2):109–115.

4. Chauhan VS, Verma A, Nayyar S, et al. Focal source and trigger mapping in atrial fibrillation: randomized controlled trial evaluating a novel adjunctive ablation strategy. *Heart Rhythm*. 2020;17(5 pt A):683-691.

5. Atienza F, Almendral J, Ormaetxe JM, et al. Comparison of radiofrequency catheter ablation of drivers and circumferential pulmonary vein isolation in atrial fibrillation: a noninferiority randomized multicenter RADAR-AF trial. *J Am Coll Cardiol*. 2014;64(23):2455–2467.

6. Tuan J, Jeilan M, Kundu S, et al. Regional fractionation and dominant frequency in persistent atrial fibrillation: effects of left atrial ablation

and evidence of spatial relationship. *Europace*. 2011;13(11):1550–1556.

7. Kumagai K, Minami K, Kutsuzawa D, Oshima S. Evaluation of the characteristics of rotational activation at high-dominant frequency and complex fractionated atrial electrogram sites during atrial fibrillation. *J Arrhythm*. 2017;33(1):49–55.

8. Roney CH, Cantwell CD, Bayer JD, et al. Spatial resolution requirements for accurate identification of drivers of atrial fibrillation. *Circ Arrhythm Electrophysiol*. 2017;10(5):e004899.

9. van der Does LJME, Yaksh A, Kik C, et al. Quest for the Arrhythmogenic Substrate of Atrial Fibrillation in Patients Undergoing Cardiac Surgery (QUASAR study): rationale and design. *J Cardiovasc Transl Res*. 2016;9(3):194–201.

10. van Staveren LN, de Groot NMS. Exploring refractoriness as an adjunctive electrical biomarker for staging of atrial fibrillation. *J Am Heart Assoc*. 2020;9(23):e018427.

11. de Groot N, van der Does L, Yaksh A, Lanters E, et al. Direct proof of endo-epicardial asynchrony of the atrial wall during atrial fibrillation in humans. *Circ Arrhythm Electrophysiol*. 2016;9(5):e003648. https://doi.org/10.1161/CIRCEP.115.003648

12. Allessie MA, de Groot NM, Houben RP, et al. Electropathological substrate of long-standing persistent atrial fibrillation in patients with structural heart disease: longitudinal dissociation. *Circ Arrhythm Electrophysiol*. 2010;3(6):606–615.

13. Lin YJ, Tai CT, Kao T, et al. Consistency of complex fractionated atrial electrograms during atrial fibrillation. *Heart Rhythm*. 2008;5(3):406–412.

14. Atienza F, Calvo D, Almendral J, et al. Mechanisms of fractionated electrograms formation in the posterior left atrium during paroxysmal atrial fibrillation in humans. *J Am Coll Cardiol*. 2011;57(9):1081–1092.

15. Jadidi AS, Duncan E, Miyazaki S, et al. Functional nature of electrogram fractionation demonstrated by left atrial high-density mapping. *Circ Arrhythm Electrophysiol*. 2012;5(1):32–42.

16. Botteron GW, Smith JM. A Technique for measurement of the extent of spatial-organization of atrial activation during atrial-fibrillation in the intact human heart. *IEEE Trans Biomed Eng*. 1995;42(6):579–586.

17. Ciaccio EJ, Biviano AB, Whang W, Wit AL, Coromilas J, Garan H. Optimized measurement of activation rate at left atrial sites with complex fractionated electrograms during atrial fibrillation. *J Cardiovasc Electrophysiol*. 2010;21(2):133–143.

18. Ciaccio EJ, Biviano AB, Whang W, Wit AL, Garan H, Coromilas J. New methods for estimating local electrical activation rate during atrial fibrillation. *Heart Rhythm*. 2009;6(1):21–32.

19. Jarman JW, Wong T, Kojodjojo P, et al. Spatiotemporal behavior of high dominant frequency during paroxysmal and persistent atrial fibrillation in the human left atrium. *Circ Arrhythm Electrophysiol*. 2012;5(4):650–658.

20. Haissaguerre M, Hocini M, Denis A, et al. Driver domains in persistent atrial fibrillation. *Circulation*. 2014;130(7):530–538.

21. de Groot NM, Houben RP, Smeets JL, et al. Electropathological substrate of longstanding persistent atrial fibrillation in patients with structural heart disease: epicardial breakthrough. *Circulation*. 2010;122(17):1674–1682.

22. Skanes AC, Mandapati R, Berenfeld O, Davidenko JM, Jalife J. Spatiotemporal periodicity during atrial fibrillation in the isolated sheep heart. *Circulation*. 1998;98(12):1236–1248.

23. Kalifa J, Tanaka K, Zaitsev AV, et al. Mechanisms of wave fractionation at boundaries of high-frequency excitation in the posterior left atrium of the isolated sheep heart during atrial fibrillation. *Circulation*. 2006;113(5):626–633.

24. Haissaguerre M, Jaïs P, Shah DC, et al. Spontaneous initiation of atrial fibrillation by ectopic beats originating in the pulmonary veins. *N Engl J Med*. 1998;339(10):659–666.

25. Allessie MA, Bonke FI, Schopman FJ. Circus movement in rabbit atrial muscle as a mechanism of tachycardia. III. The "leading circle" concept: a new model of circus movement in cardiac tissue without the involvement of an anatomical obstacle. *Circ Res*. 1977;41(1):9–18.

26. Mansour M, Mandapati R, Berenfeld O, Chen J, Samie FH, Jalife J. Left-to-right gradient of atrial frequencies during acute atrial fibrillation in the isolated sheep heart. *Circulation*. 2001;103(21):2631–2636.

27. Moe JA, Abildskov GK. Atrial fibrillation as a self-sustaining arrhythmia independent of focal discharge. *Am Heart J*. 1959;58(1):59–70.

28. Lee G, Kumar S, Teh A, et al. Epicardial wave mapping in human long-lasting persistent atrial fibrillation: transient rotational circuits, complex wavefronts, and disorganized activity. *Eur Heart J*. 2014;35(2):86–97.

29. Konings KT, Kirchhof CJ, Smeets JR, Wellens HJ, Penn OC, Allessie MA. High-density mapping of electrically induced atrial fibrillation in humans. *Circulation*. 1994;89(4):1665–1680.

30. Narayan SM, Krummen DE, Shivkumar K, Clopton P, Rappel WJ, Miller JM. Treatment of atrial fibrillation by the ablation of localized sources: CONFIRM (Conventional Ablation for Atrial Fibrillation With or Without Focal Impulse and Rotor Modulation) trial. *J Am Coll Cardiol*. 2012;60(7):628–636.

31. Lim HS, Hocini M, Dubois R, et al. Complexity and distribution of drivers in relation to duration of persistent atrial fibrillation. *J Am Coll Cardiol*. 2017;69(10):1257–1269.

32. Mandapati R, Skanes A, Chen J, Berenfeld O, Jalife J. Stable microreentrant sources as a mechanism of atrial fibrillation in the isolated sheep heart. *Circulation*. 2000;101(2):194–199.

33. Ryu K, Khrestian CM, Matsumoto N, et al. Characterization of the critical cycle length of a left atrial driver which causes right atrial fibrillatory conduction. *Conf Proc IEEE Eng Med Biol Soc*. 2004;2004:3960–3963.

34. Ryu K, Sahadevan J, Khrestian CM, Stambler BS, Waldo AL. Use of fast Fourier transform analysis of atrial electrograms for rapid characterization of atrial activation-implications for delineating possible mechanisms of atrial tachyarrhythmias. *J Cardiovasc Electrophysiol*. 2006;17(2):198–206.

35. Elvan A, Linnenbank AC, van Bemmel MW, et al. Dominant frequency of atrial fibrillation correlates poorly with atrial fibrillation cycle length. *Circ Arrhythm Electrophysiol*. 2009;2(6):634–644.

36. Houben RP, de Groot NM, Allessie MA. Analysis of fractionated atrial fibrillation electrograms by wavelet decomposition. *IEEE Trans Biomed Eng*. 2010;57(6):1388–1398.

37. Ng J, Kadish AH, Goldberger JJ. Effect of electrogram characteristics on the relationship of dominant frequency to atrial activation rate in atrial fibrillation. *Heart Rhythm*. 2006;3(11):1295–1305.

38. van Staveren LN, van der Does WFB, Heida A, Taverne YJHJ, Bogers AJJC, de Groot NMS. AF inducibility is related to conduction abnormalities at Bachmann's bundle. *J Clin Med*. 2021;10(23):5536.

39. Nitta T, van der Does WFB, Heida A, Taverne YJHJ, Bogers AJJC, de Groot NMS. Concurrent multiple left atrial focal activations with fibrillatory conduction and right atrial focal or reentrant activation as the mechanism in atrial fibrillation. *J Thorac Cardiovasc Surg*. 2004;127(3):770–778.

KEY WORDS atrial fibrillation, epicardial mapping, organized sources

APPENDIX For supplemental Methods, Results, tables, figures, and videos, please see the online version of this paper.